The 2009 IEEE/RSJ International Conference on
Intelligent Robots and Systems
October 11-15, 2009 St. Louis, USA

Base Force/Torque Sensing for Position based Cartesian Impedance Control

Christian Ott and Yoshihiko Nakamura

Abstract— **In this paper, a position based impedance controller (i.e. admittance controller) is designed by utilizing measurements of a force/torque sensor, which is mounted at the robot's base. In contrast to conventional force/torque sensing at the end-effector, placing the sensor at the base allows to implement a compliant behavior of the robot not only with respect to forces acting on the end-effector but also with respect to forces acting on the robot's structure. The resulting control problem is first analyzed in detail for the simplified one-degree-of-freedom case in terms of stability and passivity. Then, an extension to the Cartesian admittance control of a robot manipulator is discussed. Furthermore, it is shown how the steady state properties of the underlying position controller can be taken into account in the design of the outer admittance controller. Finally, a simulation study of the Cartesian admittance controller applied to a three-degrees-of-freedom manipulator is presented.**

I. INTRODUCTION

Impedance control is a prominent example for a compliant motion control algorithm used for autonomous manipulation and physical human-robot interaction [1], [2]. Different implementations of the general impedance control concept have been proposed using either impedance or admittance causality of the controller. A controller with impedance causality (sometimes called "force based impedance control") usually requires a precise torque interface and thus can benefit greatly of integrated torque sensing and torque control [3], [4]. In many commercial robots this is not feasible and only a conventional position or velocity interface is provided. In that case, a compliant behavior can still be implemented by integrating a force/torque sensor (FTS) at the end-effector and designing an outer loop admittance controller (sometimes called "position based impedance control") which provides the desired set-point for an inner loop position or velocity controller [5].

In this paper, we focus on the implementation of an admittance controller, which can be implemented on a position controlled robot. However, by using a FTS mounted at the tip of the robot, the compliant behavior can only be achieved with respect to forces acting on the end-effector, while the robot will be "insensitive" to forces acting along the robot's structure. In contrast to this, the use of robots in partly unknown human environments requires a compliant behavior of the robot also for (unplanned) contacts at different points. While the application of force sensitive skins [6] or the integration of torque sensing [7], [8] are possible approaches to handle such situations, we investigate on an alternative approach in this paper. Our approach aims at integrating a force/torque sensor at the base of the robot instead of mounting it at the end-effector. This enables to perceive forces all along the robot's structure independently of joint friction. However, since the forces measured at the base are related to the robot's motion, the manipulator dynamics must be taken into account in the design of the admittance controller.

Apart from applications to fixed mounted manipulators, we expect that the same issue will also be relevant for implementing whole body impedance controllers of humanoid robots. Feedback of the feet contact forces is often used in walking and balancing controllers of biped robots in order to control the interaction forces of the robot with the ground [9]. However, in that case the force feedback is often designed in a pragmatic way and without rigorous theoretical justification or stability analysis.

In the design of whole body impedance controllers including a compliant behavior of the lower body with respect to forces acting on the main body, we have to take account of the following key issues. Firstly, for position controlled robots it is necessary to incorporate the contact force measurements at the feet into the whole body control, since these sensors provide an indirect measurement of all forces acting on the robot. Secondly, for keeping the zero-moment-point within the support polygon of the feet, it is necessary to limit the contact forces and moments. Thirdly, for handling larger contact forces, a combination with stepping and walking technologies will be required. Within this paper, we treat the first of these problems. Compared to previous works on this problem, we aim at giving an adequate theoretical justification of the base sensor feedback by deriving all the relevant dynamic equations and by presenting a stability analysis of the one-DOF case.

The use of base mounted FTSs for identification and joint torque estimation has been well studied in the works of Dubowsky et al. [10], [11], [12]. In [11], a method for estimating the dynamical parameters of a serial manipulator arm was presented. Due to the measurement of the base force, no joint torque information was required in the identification procedure. In [12], the base FTS was used for estimating the robot's joint torques based on known dynamical parameters. The estimated torque signal was used for implementing an inner torque control loop, which was augmented by an outer

This research is partly supported by Special Coordination Funds for Promoting Science and Technology, "IRT Foundation to Support Man and Aging Society".

Ch. Ott and Y. Nakamura are with Department of Mechano-Informatics, Graduate School of Information Science and Technology, University of Tokyo, 7-3-1 Hongo, Bunkyo-ku, Tokyo 113-8656, Japan {ott,nakamura}@ynl.t.u-tokyo.ac.jp

PD position controller.

In [13], a base FTS was used in combination with a FTS mounted at the wrist for collision detection and identification in human-robot interaction tasks. Kosuge et al. [14] integrated a body force sensor on a mobile robot for cooperatively handling large objects by multiple robots.

In contrast to [12], we aim at incorporating the base force measurement directly into the design of an admittance controller instead of implementing an inner loop torque controller. The desired impedance represents a dynamic relation between external forces and the motion of the robot. This impedance will be transformed into a dynamic relation between the contact force at the base and the robot's motion. We will highlight some restrictions on the achievable closed loop dynamics which are due to the dislocation of the force sensing. A first version of the controller from this paper was already presented in [15]. In the present paper, the controller from [15] is refined by compensating for the steady state error of the underlying position controller. This refinement if achieved by modifying the outer admittance control loop based on design ideas from [16], [17].

II. Robot Model including the Base Force

In this section, the general model of a robot with n joints is discussed, in which an expression of the contact force at the base is included. In contrast to interaction forces measured at the end-effector, the forces between the robot and its base are internal forces. Therefore, we start with an extended model with a free-floating base (Fig. 1). By adding constraints on the base motion, we can derive an explicit expression of the force and torque measured at the base.

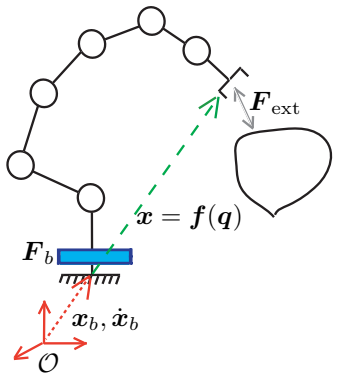

Fig. 1. Model of a robot manipulator mounted on a base FTS. The fixed base manipulator model is augmented by a free-floating base link, for which the motion will be constraint. In this way, we can represent the reaction force at the base as the constraint force.

In the following, the position and orientation of the base link is specified via local coordinates $\boldsymbol{x}_b \in \mathbb{R}^6$. The joint angles of the manipulator are denoted by $\boldsymbol{q} \in \mathbb{R}^n$. Then, the model of the robot with an free-floating base link can be written as

$$\bar{\boldsymbol{M}}(\boldsymbol{x}_b, \boldsymbol{q}) \begin{pmatrix} \ddot{\boldsymbol{x}}_b \\ \ddot{\boldsymbol{q}} \end{pmatrix} + \bar{\boldsymbol{C}}(\boldsymbol{x}_b, \dot{\boldsymbol{x}}_b, \boldsymbol{q}, \dot{\boldsymbol{q}}) \begin{pmatrix} \dot{\boldsymbol{x}}_b \\ \dot{\boldsymbol{q}} \end{pmatrix} + \bar{\boldsymbol{g}}(\boldsymbol{x}_b, \boldsymbol{q}) = \begin{pmatrix} \boldsymbol{0} \\ \boldsymbol{\tau} \end{pmatrix} - \begin{pmatrix} \boldsymbol{F}_b \\ \boldsymbol{0} \end{pmatrix} + \boldsymbol{\tau}_{\text{ext}} \ , \quad (1)$$

wherein $\bar{\boldsymbol{M}}(\boldsymbol{x}_b, \boldsymbol{q}) \in \mathbb{R}^{(6+n)\times(6+n)}$ denotes the complete inertia matrix including the base link [18]. The centrifugal and Coriolis terms are given via the matrix $\bar{\boldsymbol{C}}(\boldsymbol{x}_b, \dot{\boldsymbol{x}}_b, \boldsymbol{q}, \dot{\boldsymbol{q}}) \in \mathbb{R}^{(6+n)\times(6+n)}$. The gravity term is written as $\bar{\boldsymbol{g}}(\boldsymbol{x}_b, \boldsymbol{q}) \in \mathbb{R}^{(6+n)}$. The joint torques $\boldsymbol{\tau} \in \mathbb{R}^n$ are considered as the control inputs. The generalized force measured by the base FTS is denoted by $\boldsymbol{F}_b \in \mathbb{R}^6$. The generalized external forces (except for the generalized forces $\boldsymbol{F}_b$ exerted at the base at the location of the FTS) acting on the robot are summarized by the vector $\boldsymbol{\tau}_{\text{ext}}$. In case that the external torques are due to a generalized force $\boldsymbol{F}_{\text{ext}} \in \mathbb{R}^6$ acting at the end-effector, they can be written as

$$\boldsymbol{\tau}_{\text{ext}} = \begin{pmatrix} \boldsymbol{\tau}_{\text{ext,b}} \\ \boldsymbol{\tau}_{\text{ext,m}} \end{pmatrix} = \underbrace{\begin{bmatrix} \boldsymbol{J}_b^T(\boldsymbol{x}_b, \boldsymbol{q}) \\ \boldsymbol{J}_q^T(\boldsymbol{x}_b, \boldsymbol{q}) \end{bmatrix}}_{\boldsymbol{J}^T(\boldsymbol{x}_b, \boldsymbol{q})} \boldsymbol{F}_{\text{ext}} \ , \quad (2)$$

with $\boldsymbol{J}(\boldsymbol{x}_b, \boldsymbol{q}) \in \mathbb{R}^{(6\times(6+n))}$ as the Jacobian matrix for the serial kinematic chain from the fixed world frame $\mathcal{O}$ to the end-effector. In the following, the external torques are split up into the two components $\boldsymbol{\tau}_{\text{ext,b}} \in \mathbb{R}^6$ and $\boldsymbol{\tau}_{\text{ext,m}} \in \mathbb{R}^n$ acting on the base link and the joints, respectively.

In (1), the joint coordinates $\boldsymbol{q}$ are augmented by local coordinates of the base link motion $\boldsymbol{x}_b$ in order to incorporate the contact force $\boldsymbol{F}_b$ into the equations of motion. Since the base is attached to the ground via a stiff force/torque sensor, we have to augment (1) by an additional constraint, which prevents any motion of the base link:

$$\boldsymbol{x}_b(t) = \boldsymbol{x}_b^* \ , \quad \frac{d\boldsymbol{x}_b(t)}{dt} = \boldsymbol{0} \Rightarrow \underbrace{\begin{bmatrix} \boldsymbol{I} & \boldsymbol{0} \end{bmatrix}}_{\boldsymbol{\Phi}} \begin{pmatrix} \dot{\boldsymbol{x}}_b \\ \dot{\boldsymbol{q}} \end{pmatrix} = \boldsymbol{0} \ . \quad (3)$$

From this, one can see that the generalized force at the base $\boldsymbol{F}_b$ is represented in (1) by the Lagrangian multipliers related to the constraint matrix $\boldsymbol{\Phi} \in \mathbb{R}^{6\times(6+n)}$ from (3). In the following, this constraint will be incorporated into (1). In this way an expression of the generalized base force can be derived. Therefore, we drop the dependence on the constant position and orientation $\boldsymbol{x}_b = \boldsymbol{x}_b^*$ of the base link and write $\bar{\boldsymbol{M}}(\boldsymbol{x}_b^*, \boldsymbol{q})$, $\bar{\boldsymbol{C}}(\boldsymbol{x}_b^*, \boldsymbol{0}, \boldsymbol{q}, \dot{\boldsymbol{q}})$, and $\boldsymbol{g}(\boldsymbol{x}_b^*, \boldsymbol{q})$ in the form

$$\begin{aligned} \bar{\boldsymbol{M}}(\boldsymbol{x}_b^*, \boldsymbol{q}) &= \begin{bmatrix} \boldsymbol{M}_b(\boldsymbol{q}) & \boldsymbol{M}_c(\boldsymbol{q}) \\ \boldsymbol{M}_c^T(\boldsymbol{q}) & \boldsymbol{M}(\boldsymbol{q}) \end{bmatrix} , \\ \bar{\boldsymbol{C}}(\boldsymbol{x}_b^*, \boldsymbol{0}, \boldsymbol{q}, \dot{\boldsymbol{q}}) &= \begin{bmatrix} \boldsymbol{C}_b(\boldsymbol{q}, \dot{\boldsymbol{q}}) & \boldsymbol{C}_1(\boldsymbol{q}, \dot{\boldsymbol{q}}) \\ \boldsymbol{C}_2(\boldsymbol{q}, \dot{\boldsymbol{q}}) & \boldsymbol{C}(\boldsymbol{q}, \dot{\boldsymbol{q}}) \end{bmatrix} , \\ \bar{\boldsymbol{g}}(\boldsymbol{x}_b^*, \boldsymbol{q}) &= \begin{pmatrix} \boldsymbol{g}_b(\boldsymbol{q}) \\ \boldsymbol{g}(\boldsymbol{q}) \end{pmatrix} , \end{aligned}$$

where $\boldsymbol{M}(\boldsymbol{q}) \in \mathbb{R}^{n\times n}$ is the joint level inertia matrix and $\boldsymbol{M}_c(\boldsymbol{q}) \in \mathbb{R}^{(6\times n)}$ represents the inertia coupling matrix between the manipulator and the base link. Notice that the classical robot dynamics can be obtained by pre-multiplying (1) by a matrix spanning the left nullspace of $\boldsymbol{\Phi}^T$:

$$\boldsymbol{M}(\boldsymbol{q})\ddot{\boldsymbol{q}} + \boldsymbol{C}(\boldsymbol{q}, \dot{\boldsymbol{q}})\dot{\boldsymbol{q}} + \boldsymbol{g}(\boldsymbol{q}) = \boldsymbol{\tau} + \boldsymbol{\tau}_{\text{ext,m}} \ . \quad (4)$$

In order to get an expression for the base force as a function of the robot's motion, we instead pre-multiply (1)

by $\mathbf{\Phi}$ and obtain

$$\boldsymbol{F}_b = \boldsymbol{\tau}_{\text{ext,b}} - \boldsymbol{M}_c(\boldsymbol{q})\ddot{\boldsymbol{q}} - \boldsymbol{C}_1(\boldsymbol{q},\dot{\boldsymbol{q}})\dot{\boldsymbol{q}} - \boldsymbol{g}_b(\boldsymbol{q}) \ . \tag{5}$$

Moreover, substituting $\ddot{\boldsymbol{q}}$ from (4) into (5), leads to

$$\begin{aligned}\boldsymbol{F}_b = &-\boldsymbol{M}_c(\boldsymbol{q})\boldsymbol{M}^{-1}(\boldsymbol{q})[\boldsymbol{\tau} + \boldsymbol{\tau}_{\text{ext,m}} - \boldsymbol{C}(\boldsymbol{q},\dot{\boldsymbol{q}})\dot{\boldsymbol{q}} \\ &-\boldsymbol{g}(\boldsymbol{q})] + \boldsymbol{\tau}_{\text{ext,b}} - \boldsymbol{C}_1(\boldsymbol{q},\dot{\boldsymbol{q}})\dot{\boldsymbol{q}} - \boldsymbol{g}_b(\boldsymbol{q}) \ .\end{aligned} \tag{6}$$

The last three equations (4)-(6) basically represent three relations between $\ddot{\boldsymbol{q}}$, $\boldsymbol{\tau}$, and $\boldsymbol{F}_b$, which will be relevant for the derivation and analysis of the admittance controller:

A: (4) represents a relation $\ddot{\boldsymbol{q}} \rightleftharpoons \boldsymbol{\tau}$ (robot dynamics).
B: (5) represents a relation $\boldsymbol{F}_b \rightleftharpoons \ddot{\boldsymbol{q}}$.
C: (6) represents a relation $\boldsymbol{F}_b \rightleftharpoons \boldsymbol{\tau}$.

From (5) and (6), it is obvious that the base force, which is measured by the FTS, depends not only on the robot's state $(\boldsymbol{q},\dot{\boldsymbol{q}})$ and the generalized external forces $\boldsymbol{\tau}_{\text{ext}}$, but also on the current joint torque $\boldsymbol{\tau}$, which is considered as the control input in our case. It should be mentioned that therefore the use of this force in the controller is from a theoretical point of view not unproblematic. This issue basically arises because we ignore the force sensor's elasticity in the model and treat it as an ideal force sensing element. However, for the controller design, one should avoid direct feedback from the force sensor measurement to the joint torque output of the controller as this feedback would not be well-defined.

III. Controller design: The One-DOF case

In this paper, we focus on an admittance controller design. Therefore, we will use an underlying position controller for the robot manipulator and design a compliant impedance behavior in an outer loop based on the measured forces at the base. For this, in particular the relation between the external forces and the measured contact force at the base is of interest. The general relations for the n degrees-of-freedom case are given in (5) and (6). Before discussing the design of a Cartesian admittance controller in section IV, we will analyze the simple one-degree-of-freedom case in this section in order to clarify the main design issues based on a simple model.

Consider the model shown in Fig. 2, in which a single mass M is controlled via an actuator force F. Compared to the general model described in Section II, we have the correspondence as shown in Tab. I. The actuator force F is determined by the output of an inner loop position controller for $x \in \mathbb{R}$, which gets its set-point x_d from an outer admittance controller. In the analysis of this section, we will assume that the underlying position controller has the form of a PD controller with velocity feed-forward term, i.e.

$$F = -P(x - x_d) - D(\dot{x} - \dot{x}_d) \ , \tag{7}$$

with positive PD controller gains $P > 0$ and $D > 0$.

It can easily be verified that in this simple one-DOF case the complete inertia matrix becomes

$$\bar{\boldsymbol{M}} = \begin{bmatrix} M_b + M & M \\ M & M \end{bmatrix} \ .$$

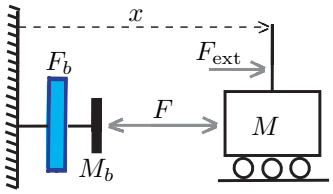

Fig. 2. Model of single mass, actuated by the force F and mounted on a base force sensor.

TABLE I
Correspondence between the general and the one-degrees-of-freedom case

	general case	one-DOF
Coordinates	$\boldsymbol{q}$	x
Actuator force	$\boldsymbol{\tau}$	F
External force	$\boldsymbol{F}_{\text{ext}}$	F_{ext}
	$\boldsymbol{\tau}_{\text{ext,b}}$	F_{ext}
	$\boldsymbol{\tau}_{\text{ext,m}}$	F_{ext}

and thus the inertia coupling matrix $\boldsymbol{M}_c(\boldsymbol{q})$ is given by M. By evaluating (4)-(6) for this one-DOF case, we obtain

$$\text{(A)} \quad M\ddot{x} = F + F_{\text{ext}} \ , \tag{8}$$

$$\text{(B)} \quad F_b = F_{\text{ext}} - M\ddot{x} \ , \tag{9}$$

$$\text{(C)} \quad F_b = -F \ . \tag{10}$$

Due to $\boldsymbol{M}_c(\boldsymbol{q}) \hat{=} M$, the relation between F_b and the actuator force F in (10) has a very simple form, i.e. the measured base force is equal to the reaction force of the actuator.

As a control goal, we assume a desired impedance relation in form of a second-order mass-spring-damper system

$$M_d\ddot{x} + D_d\dot{x} + K_d(x - x_0) = F_{\text{ext}} \ , \tag{11}$$

with $M_d > 0$, $D_d > 0$, and $K_d > 0$ as the desired inertia, damping, and stiffness, respectively. The point $x_0 \in \mathbb{R}$ is the virtual equilibrium position and is assumed constant. The desired behavior (11) defines a dynamic relation between $\dot{x}$ and the external force F_{ext}. Since we want to realize this behavior based on the measurement of the contact force at the base, we transform the desired impedance into a relation between $\dot{x}$ and the base force F_b. This can be done by combining (11) and (9) to obtain

$$(M_d - M)\ddot{x} + D_d\dot{x} + K_d(x - x_0) = F_b \ . \tag{12}$$

From (12), one can see that the target inertia M_d must always be larger than M, otherwise (12) would result in an unstable dynamics. Notice that (12) is independent of the underlying position controller (7) used for the implementation via admittance control. For an ideal position controller, the actual position x would become identical to its reference motion x_d. One possible way for implementing (11) with a position controlled robot is then to replace x in (12) by x_d:

$$(M_d - M)\ddot{x}_d + D_d\dot{x}_d + K_d(x_d - x_0) = F_b \ . \tag{13}$$

This design strategy, shown in Fig. 3 so far did not involve the particular form of the underlying position controller.

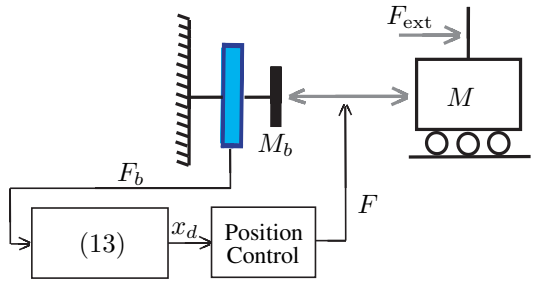

Fig. 3. Admittance control of the one-DOF model using a FTS at the base. If the admittance controller from (13) is replaced by (18), one can take account of the static error resulting from the position controller.

However, for analyzing the stability properties we need to consider a particular controller structure. In the following, we assume the PD controller (7). Then, the closed loop system can be obtained from (8) and (13). By using (7) and (10), we can eliminate F and F_b from (8) and (13) to obtain

$$M\ddot{x} + D(\dot{x} - \dot{x}_d) + P(x - x_d) = F_{\text{ext}} \ , \tag{14}$$

$$(M_d - M)\ddot{x}_d + D_d\dot{x}_d + K_d(x_d - x_0) = P(x - x_d) + D(\dot{x} - \dot{x}_d) \ . \tag{15}$$

Let us first analyze the equilibrium points of the system. Therefore, we assume that a constant external force F_{ext} is acting on the system. Then the unique equilibrium point $(\hat{x}, \hat{x}_d)$ can be obtained from (14)-(15) as

$$\hat{x}_d = x_0 + \frac{1}{K_d}F_{\text{ext}} \tag{16}$$

$$\hat{x} = x_0 + \frac{K_d + P}{K_d P}F_{\text{ext}} \ . \tag{17}$$

Using the new coordinates $\tilde{x} = x - \hat{x}$ and $\tilde{x}_d = x_d - \hat{x}_d$, the stability of the equilibrium point in the sense of Lyapunov can be shown based on the Lyapunov function

$$V(\tilde{x}, \tilde{x}_d, \dot{\tilde{x}}, \dot{\tilde{x}}_d) = \frac{1}{2}\begin{pmatrix}\dot{\tilde{x}}\\ \dot{\tilde{x}}_d\end{pmatrix}^T \begin{bmatrix}M & 0\\ 0 & (M_d - M)\end{bmatrix}\begin{pmatrix}\dot{\tilde{x}}\\ \dot{\tilde{x}}_d\end{pmatrix} + \frac{1}{2}\begin{pmatrix}\tilde{x}\\ \tilde{x}_d\end{pmatrix}^T \begin{bmatrix}P & -P\\ -P & P + K_d\end{bmatrix}\begin{pmatrix}\tilde{x}\\ \tilde{x}_d\end{pmatrix} \ ,$$

which is positive definite for $M_d > M$. The time derivative of this function along the solutions of (14)-(15) is given by

$$\dot{V}(\tilde{x}, \tilde{x}_d, \dot{\tilde{x}}, \dot{\tilde{x}}_d) = -D_d\dot{\tilde{x}}_d^2 - D(\dot{\tilde{x}} - \dot{\tilde{x}}_d)^2 \ ,$$

from which stability of the equilibrium point follows. Moreover, by invoking La'Salle's invariance principle [19], also asymptotical stability can be shown.

In the stability analysis, a constant external force was assumed. Regarding interaction with dynamic environments, one can additionally show passivity of the closed loop system with the external force F_{ext} as input and the velocity $\dot{x}$ as output. This can be verified by considering the storage function

$$V(x, x_d, \dot{x}, \dot{x}_d) = \frac{1}{2}M\dot{x}^2 + \frac{1}{2}(M_d - M)\dot{x}_d^2 + \frac{1}{2}P(x - x_d)^2 + \frac{1}{2}K_d(x_d - x_0)^2 \ ,$$

for which the time derivative along the solutions of (14)-(15) is given by

$$\dot{V}(x, x_d, \dot{x}, \dot{x}_d) = -D_d\dot{x}_d^2 - D(\dot{x} - \dot{x}_d)^2 + \dot{x}F_{\text{ext}} \ .$$

From this, the passivity of the system with respect to the input-output pair $(\dot{x}, F_{\text{ext}})$ follows immediately[1].

Notice that in the controller design so far, the outer loop admittance controller (13) was designed independently of the inner position controller. For a non-ideal position controller, the achieved impedance (as a relation between x and F_{ext}) will be slightly distorted according to the properties of the inner loop position controller. In case of the PD controller (7), one can see from the steady state equation (17) that the achieved steady state behavior corresponds to a stiffness value of $K_dP/(K_d + P)$. This stiffness tends to the desired value K_d for large position controller gains $P >> K_d$. However, it is possible to exactly compensate for the steady state error of the position controller if the gain P of the position controller is known. Then the stiffness term of the outer admittance control loop can be modified by adopting the techniques used in [16], [17]. If the stiffness term in (13) is replaced by $\frac{K_dP}{P - K_d}(x_d - x_0)$, with $K_d < P$, the desired stiffness K_d is achieved exactly. However, in this case the position controller gain P poses an upper limit for the achievable stiffness $K_d < P$. The modified admittance controller is then given by

$$(M_d - M)\ddot{x}_d + D_d\dot{x}_d + \frac{K_dP}{P - K_d}(x_d - x_0) = F_b \ . \tag{18}$$

Notice that this modification would not be necessary if instead of the underlying PD controller a controller with integral action is used.

IV. Cartesian admittance control of a multi-body robot

In the previous section, the admittance controller design and its stability analysis have been presented in detail for a simple model. In this section, the same line of argumentation will be followed for designing a Cartesian admittance controller of a multi-body robot manipulator.

Let the desired impedance be defined in Cartesian coordinates $\boldsymbol{x} = \boldsymbol{f}(\boldsymbol{q}) \in \mathbb{R}^6$, $\dot{\boldsymbol{x}} = \boldsymbol{J}(\boldsymbol{q})\dot{\boldsymbol{q}}$, where $\boldsymbol{f}(\boldsymbol{q})$ represents the forward kinematic mapping and $\boldsymbol{J}(\boldsymbol{q}) \in \mathbb{R}^{(6\times 6)}$ the analytic Jacobian $\boldsymbol{J}(\boldsymbol{q}) := \partial\boldsymbol{f}(\boldsymbol{q})/\partial\boldsymbol{q}$. In the following derivations, we will consider the non-redundant case and assume that the Jacobian is non-singular (and thus invertible) in the relevant workspace. Extensions to the redundant case would additionally require to consider the effect of the nullspace dynamics (see, e.g., [21], [22]) on the measurement of the base FTS.

As a desired impedance, we assume a mass-spring-damper-like system of the form

$$\boldsymbol{\Lambda}_d\ddot{\boldsymbol{x}} + \boldsymbol{D}_d\dot{\boldsymbol{x}} + \boldsymbol{K}_d(\boldsymbol{x} - \boldsymbol{x}_0) = \boldsymbol{F}_{\text{ext}} \ , \tag{19}$$

[1]A sufficient condition for a system (with input $\boldsymbol{u}$ and output $\boldsymbol{y}$) to be passive [20] is given by the existence of a continuous storage function S which is bounded from below and for which the derivative with respect to time along the solutions of the system satisfies the inequality $\dot{S} \leq \boldsymbol{y}^T\boldsymbol{u}$.

with the symmetric and positive definite matrices $\boldsymbol{\Lambda}_d \in \mathbb{R}^{6\times6}$, $\boldsymbol{D}_d \in \mathbb{R}^{6\times6}$, and $\boldsymbol{K}_d \in \mathbb{R}^{6\times6}$ representing the desired inertia, damping, and stiffness, respectively. The virtual equilibrium position is given by $\boldsymbol{x}_0 \in \mathbb{R}^6$.

The main advantage of using the base sensor is that it allows to measure forces all along the robot's structure, not only the the end-effector. Still, the above desired impedance is defined with respect to Cartesian coordinates describing the end-effector position and orientation. This means that for forces exerted in the vicinity of the end-effector, the perceived impedance will be close to (19). If the external forces are exerted far away from the end-effector, e.g. close to the base link, then the perceived impedance behavior will be different. However, under the assumption that a reliable contact point estimation is feasible, one could aim at adapting the compliance behavior to the current point of contact.

In order to compare the desired impedance with the equations of motion (4) and for combining it with (5)-(6), we rewrite the model (4) in Cartesian coordinates as[2]

$$\boldsymbol{\Lambda}(\boldsymbol{q})\ddot{\boldsymbol{x}} + \boldsymbol{\mu}(\boldsymbol{q},\dot{\boldsymbol{q}})\dot{\boldsymbol{x}} + \boldsymbol{p}(\boldsymbol{q}) = \boldsymbol{J}^{-T}(\boldsymbol{q})\boldsymbol{\tau} + \boldsymbol{F}_{\text{ext}} \ , \qquad (20)$$

where $\boldsymbol{\Lambda}(\boldsymbol{q})$ denotes the Cartesian inertia matrix $\boldsymbol{\Lambda}(\boldsymbol{q}) = (\boldsymbol{J}(\boldsymbol{q})\boldsymbol{M}^{-1}(\boldsymbol{q})\boldsymbol{J}^T(\boldsymbol{q}))^{-1}$ and the matrices $\boldsymbol{\mu}(\boldsymbol{q},\dot{\boldsymbol{q}})$ and the Cartesian gravity term $\boldsymbol{p}(\boldsymbol{q})$ are given by $\boldsymbol{\mu}(\boldsymbol{q},\dot{\boldsymbol{q}}) = \boldsymbol{J}^{-T}(\boldsymbol{q})(\boldsymbol{C}(\boldsymbol{q},\dot{\boldsymbol{q}}) - \boldsymbol{M}(\boldsymbol{q})\boldsymbol{J}^{-1}(\boldsymbol{q})\dot{\boldsymbol{J}}(\boldsymbol{q}))\boldsymbol{J}^{-1}(\boldsymbol{q})$ and $\boldsymbol{p}(\boldsymbol{q}) = \boldsymbol{J}^{-T}(\boldsymbol{q})\boldsymbol{g}(\boldsymbol{q})$, respectively.

The relation between the base force and the accelerations, i.e. (5), becomes

$$\boldsymbol{F}_b = \boldsymbol{J}_b^T(\boldsymbol{q})\boldsymbol{F}_{\text{ext}} - \boldsymbol{\Lambda}_c(\boldsymbol{q})\ddot{\boldsymbol{x}} - \boldsymbol{\mu}_1(\boldsymbol{q},\dot{\boldsymbol{q}})\dot{\boldsymbol{x}} - \boldsymbol{g}_b(\boldsymbol{q}) \ , \qquad (21)$$

where the inertia coupling matrix $\boldsymbol{\Lambda}_c(\boldsymbol{q})$ and $\boldsymbol{\mu}_1(\boldsymbol{q},\dot{\boldsymbol{q}})$ are given by $\boldsymbol{\Lambda}_c(\boldsymbol{q}) = \boldsymbol{M}_c(\boldsymbol{q})\boldsymbol{J}^{-1}(\boldsymbol{q})$ and $\boldsymbol{\mu}_1(\boldsymbol{q},\dot{\boldsymbol{q}}) = (\boldsymbol{C}_1(\boldsymbol{q},\dot{\boldsymbol{q}}) - \boldsymbol{M}_c(\boldsymbol{q})\boldsymbol{J}^{-1}(\boldsymbol{q})\dot{\boldsymbol{J}}(\boldsymbol{q}))\boldsymbol{J}^{-1}(\boldsymbol{q})$, respectively.

Finally, equation (6) takes the form

$$\begin{aligned}\boldsymbol{F}_b = \boldsymbol{M}_c(\boldsymbol{q})\boldsymbol{M}^{-1}(\boldsymbol{q})[\boldsymbol{\tau} + \boldsymbol{J}_m^T(\boldsymbol{q})\boldsymbol{F}_{\text{ext}} - \boldsymbol{\mu}(\boldsymbol{q},\dot{\boldsymbol{q}})\dot{\boldsymbol{x}} \\ -\boldsymbol{p}(\boldsymbol{q})] + \boldsymbol{J}_b^T(\boldsymbol{q})\boldsymbol{F}_{\text{ext}} - \boldsymbol{\mu}_1(\boldsymbol{q},\dot{\boldsymbol{q}})\dot{\boldsymbol{x}} - \boldsymbol{g}_b(\boldsymbol{q}) \ .\end{aligned} \qquad (22)$$

Similar to the procedure in the one-DOF case, we transform the desired impedance (19), which represents a relation between the Cartesian velocity and the external forces, into an impedance relation between the velocity and the generalized base force. Therefore, we utilize (21) to obtain

$$\begin{aligned}\left(\boldsymbol{\Lambda}_d - \boldsymbol{J}_b^{-T}(\boldsymbol{q})\boldsymbol{\Lambda}_c(\boldsymbol{q})\right)\ddot{\boldsymbol{x}} + \\ \left(\boldsymbol{D}_d - \boldsymbol{J}_b^{-T}(\boldsymbol{q})\boldsymbol{\mu}_1(\boldsymbol{q},\dot{\boldsymbol{q}})\right)\dot{\boldsymbol{x}} + \\ \boldsymbol{K}_d(\boldsymbol{x} - \boldsymbol{x}_0) = \boldsymbol{J}_b(\boldsymbol{q})^{-T}(\boldsymbol{F}_b + \boldsymbol{g}_b(\boldsymbol{q})).\end{aligned} \qquad (23)$$

Equation (23) presents the main component for the design of the controller. We are aiming again at an admittance controller with an inner position control loop. Instead of implementing the underlying position controller based on the Cartesian dynamics (20), a joint level position controller can be used and combined with the Cartesian admittance by inverse kinematics as shown in Fig. 4. Let $\boldsymbol{x}_d \in \mathbb{R}^n$ be the desired Cartesian position resulting from the admittance controller and $\boldsymbol{q}_d = \boldsymbol{f}^{-1}(\boldsymbol{x}_d)$ the corresponding set-point for the position controller, the admittance controller, which implements (19) based on the measurement of the base force, can be written as

$$\begin{aligned}\left(\boldsymbol{\Lambda}_d - \boldsymbol{J}_b^{-T}(\boldsymbol{q}_d)\boldsymbol{\Lambda}_c(\boldsymbol{q}_d)\right)\ddot{\boldsymbol{x}}_d + \\ \left(\boldsymbol{D}_d - \boldsymbol{J}_b^{-T}(\boldsymbol{q}_d)\boldsymbol{\mu}_1(\boldsymbol{q}_d,\dot{\boldsymbol{q}}_d)\right)\dot{\boldsymbol{x}}_d + \\ \boldsymbol{K}_d(\boldsymbol{x}_d - \boldsymbol{x}_0) = \boldsymbol{J}_b^{-T}(\boldsymbol{q}_d)(\boldsymbol{F}_b + \boldsymbol{g}_b(\boldsymbol{q}_d)).\end{aligned} \qquad (24)$$

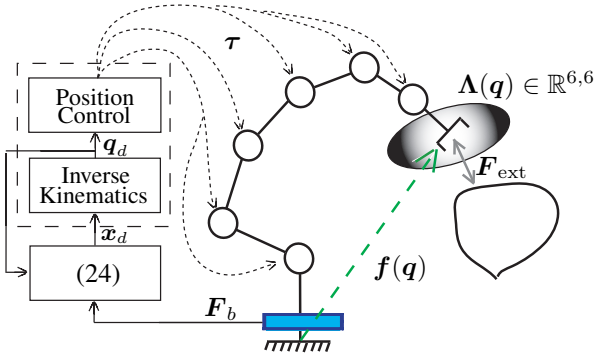

Fig. 4. Cartesian admittance control of a manipulator mounted on a base FTS. If the admittance controller from (24) is replaced by (28), one can take account of the static error resulting from the underlying position controller.

Similar to the one-DOF case, a correction of the steady state error due to a non-ideal position controller is possible by modification of the stiffness term in (24). Therefore, it is required that the steady state properties of the controller are known. If we consider for instance a PD controller with gravity compensation

$$\boldsymbol{\tau} = \boldsymbol{P}(\boldsymbol{q}_d - \boldsymbol{q}) + \boldsymbol{D}(\dot{\boldsymbol{q}}_d - \dot{\boldsymbol{q}}) + \boldsymbol{g}(\boldsymbol{q}) \ , \qquad (25)$$

with positive definite gain matrices $\boldsymbol{P} \in \mathbb{R}^{n\times n}$ and $\boldsymbol{D} \in \mathbb{R}^{n\times n}$, then the steady state error for a constant external force $\boldsymbol{F}_{\text{ext}}$ depends on the proportional gain matrix $\boldsymbol{P}$. In steady state, the joint angle $\hat{\boldsymbol{q}}$ clearly fulfills

$$\hat{\boldsymbol{\tau}} = \boldsymbol{P}(\boldsymbol{q}_d - \hat{\boldsymbol{q}}) = -\boldsymbol{J}^T(\hat{\boldsymbol{q}})\boldsymbol{F}_{\text{ext}} \ . \qquad (26)$$

The correction of the admittance control law can be done by following the methods proposed in [16], [17]. From (19) one can see that in the steady state of the desired impedance, the condition $\boldsymbol{K}_d(\boldsymbol{f}(\hat{\boldsymbol{q}}) - \boldsymbol{x}_0) = \boldsymbol{F}_{\text{ext}}$ should hold. By combining this equation with (26), we get

$$\boldsymbol{P}(\boldsymbol{q}_d - \hat{\boldsymbol{q}}) = -\boldsymbol{J}^T(\hat{\boldsymbol{q}})\boldsymbol{K}_d(\boldsymbol{f}(\hat{\boldsymbol{q}}) - \boldsymbol{x}_0) \ . \qquad (27)$$

The idea, adopted from [16], [17], is then to solve (27) for $\hat{\boldsymbol{q}}$ and use the resulting function $\hat{\boldsymbol{q}}(\boldsymbol{q}_d, \boldsymbol{x}_0)$ in the implementation of the admittance. In this way, we obtain

$$\begin{aligned}\left(\boldsymbol{\Lambda}_d - \boldsymbol{J}_b^{-T}(\boldsymbol{q}_d)\boldsymbol{\Lambda}_c(\boldsymbol{q}_d)\right)\ddot{\boldsymbol{x}}_d + \\ \left(\boldsymbol{D}_d - \boldsymbol{J}_b^{-T}(\boldsymbol{q}_d)\boldsymbol{\mu}_1(\boldsymbol{q}_d,\dot{\boldsymbol{q}}_d)\right)\dot{\boldsymbol{x}}_d + \\ \boldsymbol{K}_d(\boldsymbol{f}(\hat{\boldsymbol{q}}(\boldsymbol{q}_d,\boldsymbol{x}_0)) - \boldsymbol{x}_0) = \boldsymbol{J}_b^{-T}(\boldsymbol{q}_d)(\boldsymbol{F}_b + \boldsymbol{g}_b(\boldsymbol{q}_d)).\end{aligned} \qquad (28)$$

[2]While the assumptions made in this section would formally allow to represent the system dynamics in terms of $\boldsymbol{x} = \boldsymbol{f}^{-1}(\boldsymbol{q})$ and $\dot{\boldsymbol{x}}$ only, we keep the dependence of the dynamic equations on the joint angles $\boldsymbol{q}$ since this formulation is closer to the actual implementation of the control law.

More details on how to solve an equation like (27) for $\hat{\boldsymbol{q}}$ can be found in [16], [17]. However, this solution requires that the controller gain $\boldsymbol{P}$ is "larger" than the Cartesian stiffness $\boldsymbol{K}_d$, i.e. (27) can be solved uniquely only if $\boldsymbol{J}^T(\boldsymbol{q})\boldsymbol{K}_d\boldsymbol{J}(\boldsymbol{q}) < \boldsymbol{P}$ holds. Thus, the gain of the position controller represents an upper bound for the achievable stiffness, which is not surprising at all.

V. Simulation Results

For the verification of the controller from Fig. 4, we present a simulation study of a planar three-degrees-of-freedom robot as shown in Fig. 5. For the inner loop position controller a PD controller with gravity compensation as in (25) is used. The proportional gain matrix $\boldsymbol{P}$ is chosen as a diagonal matrix. The two sets of proportional gains, which have been used in the simulations, are given in Tab. II. For the design of the damping gain matrix $\boldsymbol{D}$ the "double diagonalization design" from [23] with a damping factor of 0.7 is applied resulting in a configuration dependent damping matrix.

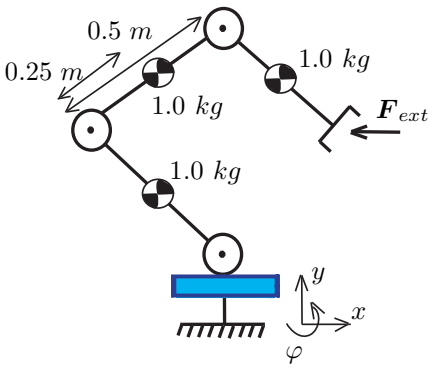

Fig. 5. Simulation model: A planar three-DOF manipulator mounted on a base FTS. The link length of all three segments is set to 0.5m. The inertia of the links is represented by a single mass located in the center of the link segments. The external force acts in the horizontal x-direction. As Cartesian coordinates, the end-effector position (x, y) and orientation ϕ are used.

TABLE II

Gains of the joint position controller

Joint	1	2	3
Prop. Gain "L" $[Nm/rad]$	$5\ 10^3$	$5\ 10^3$	10^3
Prop. Gain "H" $[Nm/rad]$	$5\ 10^4$	$5\ 10^4$	10^4

TABLE III

Impedance Parameters

Direction	x	y	φ
Inertia	$5\ Ns^2/m$	$5\ Ns^2/m$	$5\ Nms^2/rad$
Stiffness	$100\ N/m$	$100\ N/m$	$10\ Nm/rad$
Damping	$31.3\ Ns/m$	$31.3\ Ns/m$	$9.9\ Nms/rad$

In this simulation study, we compare the two admittance controllers based on (24) and on (28) and we will observe the influence of the underlying position controller on the closed loop behavior. In all simulations, the desired impedance is chosen according to (19) with diagonal matrices for the desired inertia, damping, and stiffness. The values of the diagonal elements are given in Tab. III. The external excitation is chosen as a stepwise external force acting on the end-effector in x-direction (see Fig. 5).

In the first simulation, we use the admittance controller from (24) and the parameter set "L" from Tab. II. The initial configuration for the simulation can be seen in Fig. 5. The resulting step response for a force step of $1N$ in x-direction is shown in Fig. 6. The desired step response in x-direction according to the parameters in Tab. III is shown by the black dotted line, while the simulation result is shown by the black solid line. While the transient behavior is similar to the desired behavior, one can observe a steady-state error, which results from the non-ideal position controller with a finite proportional gain $\boldsymbol{P}$. This can also be seen by observing the motion in y- and ϕ-direction, which should remain zero according to the desired behavior.

In the second simulation, we now replace the admittance control law (24) by (28). In order to solve (27) for $\hat{\boldsymbol{q}}(\boldsymbol{q}_d, \boldsymbol{q}_0)$, a first order approximation is used. The results are shown in Fig. 7. One can see that the modified stiffness term in the admittance controller eliminates the steady state error due to the position controller. Clearly, for the implementation of (28) it must be assumed that the value of the proportional gain of the underlying position controller is known. In the transient phase, the quality of the position controller still influences the accuracy. The deviation of the Cartesian coordinates in y- and ϕ-direction from the equilibrium during the transient phase can be explained by the effects of a non-ideal underlying joint position controller. This is verified by a third simulation in which the admittance controller (28) is combined with a joint position controller with higher gains, which are given by the set "H" in Tab. II. The corresponding simulation result is shown in Fig. 8. One can see that for the higher proportional gains in the position controller the desired impedance is realized much better during the transient phase.

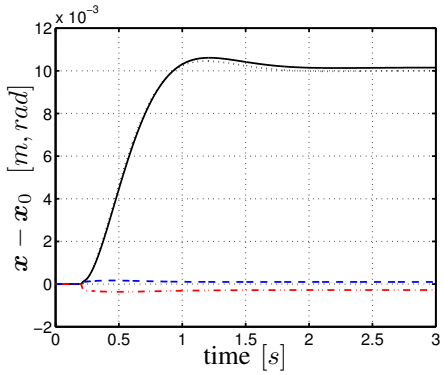

Fig. 6. Simulation result with the admittance controller (24) and an underlying position controller with the lower proportional gains (set "L" in Tab. II). The desired step response in x-direction is given by the black dotted line. The simulation result for the Cartesian motion in x-, y-, and ϕ-direction are shown by the black solid line, the blue dashed line and the red dashed-dotted line, respectively.

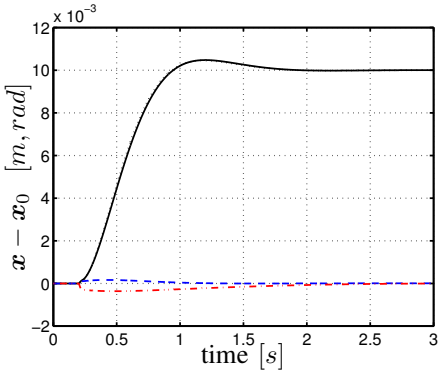

Fig. 7. Simulation result with the admittance controller (28) and an underlying position controller with the lower proportional gains (set "L" in Tab. II). The desired step response in x-direction is given by the black dotted line. The simulation result for the Cartesian motion in x-, y-, and ϕ-direction are shown by the black solid line, the blue dashed line and the red dashed-dotted line, respectively.

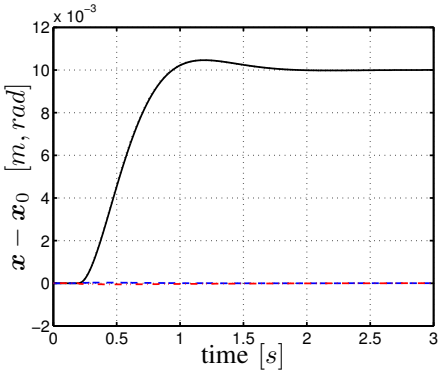

Fig. 8. Simulation result with the admittance controller (28) and an underlying position controller with the higher proportional gains (set "H" in Tab. II). The desired step response in x-direction is given by the black dotted line. The simulation result for the Cartesian motion in x-, y-, and ϕ-direction are shown by the black solid line, the blue dashed line and the red dashed-dotted line, respectively.

VI. Summary and Outlook

In this paper, we analyzed the admittance control problem of a robot manipulator, in which the force/torque sensor is mounted at the base of the robot. This has the advantage that external forces acting all along the robot's structure are perceived by the sensor. The desired impedance still is given in terms of a dynamic relation between external forces at the tip and the end-effector motion, but the interaction of the robot with its environment is not restricted to the end-effector. The contribution of this paper is a generalization of the controller from [15] by taking the steady state properties of the underlying position controller into account in the design of the outer admittance control loop. The design idea was exemplified by a detailed analysis of the one-DOF case. The Cartesian impedance control problem for a general multi-degrees-of-freedom robot was discussed and verified by a simulation study. We believe that the analysis can also be useful for implementing whole body impedance and compliance controllers of legged robotic systems in which the ground reaction forces of the feet are measured by force/torque sensors.

References

[1] N. Hogan, "Impedance control: An approach to manipulation, part I - theory," *ASME Journal of Dynamic Systems, Measurement, and Control*, vol. 107, pp. 1–7, 1985.

[2] A. D. Santis, B. Siciliano, A. D. Luca, and A. Bicchi, "An atlas of physical human–robot interaction," *Mechanism and Machine Theory*, vol. 43, pp. 253–270, March 2008.

[3] J. Luh, W. Fisher, and R. Paul, "Joint torque control by a direct feedback for industrial robots," *IEEE Transactions on Automatic Control*, vol. 28, no. 2, pp. 153–161, 1983.

[4] G. Hirzinger, N. Sporer, A. Albu-Schäffer, M. Hähnle, R. Krenn, A. Pascucci, and M. Schedl, "DLR's torque-controlled light weight robot III - are we reaching the technological limits now?" in *IEEE Int. Conf. on Robotics and Automation*, 2002, pp. 1710–1716.

[5] B. Siciliano, L. Sciavicco, L. Villani, and G. Oriolo, *Robotics: Modelling, Planning and Control*, ser. Advanced Textbooks in Control and Signal Processing. Springer-Verlag, 2009.

[6] M. Lee and H. Nicholls, "Tactile sensing for mechatronics: a state of the art survey," *Mechatronics*, vol. 9, no. 1, pp. 1–31, 1999.

[7] Ch. Ott, O. Eiberger, W. Friedl, B. Bäuml, U. Hillenbrand, Ch. Borst, A. Albu-Schäffer, B. Brunner, H. Hirschmüller, S. Kielhöfer, R. Konietschke, M. Suppa, T. Wimböck, F. Zacharias, and G. Hirzinger, "A humanoid two-arm system for dexterous manipulation," in *IEEE-RAS International Conference on Humanoid Robots*, 2006, pp. 276–283.

[8] G. Cheng, S.-H. Hyon, J. Morimoto, A. Ude, G. Colvin, W. Scroggin, and S. Jacobsen, "Cb: A humanoid research platform for exploring neuroscience," in *IEEE-RAS International Conference on Humanoid Robots*, 2006, pp. 182–187.

[9] S. Kajita, *Humanoid Robot*. Ohmsha, 2005, (in Japanese).

[10] H. West, E. Papadopoulos, S. Dubowsky, and H. Cheah, "A method for estimating the mass properties of a manipulator bymeasuring the reaction moments at its base," in *IEEE Int. Conf. on Robotics and Automation*, 1989, pp. 1510–1516.

[11] G. Liu, K. Iagnemma, S. Dubowsky, and G. Morel, "A base force/torque sensor approach to robot manipulator inertial parameter estimation," in *IEEE Int. Conf. on Robotics and Automation*, 1998, pp. 3316–3321.

[12] G. Morel, K. Iagnemma, and S. Dubowsky, "The precise control of manipulators with high joint-friction using base force/torque sensing," *Automatica*, vol. 36, no. 7, pp. 931–941, 2000.

[13] S. Lu, J. Chung, and S. A. Velinsky, "Human-robot collosion detection and identification based on wrist and base force/torque sensors," in *IEEE/RSJ Int. Conf. on Intelligent Robots and Systems*, 2005, pp. 3796–3801.

[14] K. Kosuge, T. Oosumi, Y. Hirata, H. Asama, H. Kaetsu, and K. Kowabata, "Handling of a single object by multiple autonomous mobile robots in coordination with body force sensor," in *IEEE/RSJ Int. Conf. on Intelligent Robots and Systems*, 1998, pp. 1419–1424.

[15] Ch. Ott and Y. Nakamura, "Admittance control using a base force/torque sensor," in *International IFAC Symposium on Robot Control (SYROCO)*, 2009.

[16] A. Albu-Schäffer, Ch. Ott, and G. Hirzinger, "Passivity based cartesian impedance control for flexible joint manipulators," in *IFAC Symposium on Nonlinear Control Systems*, 2004.

[17] Ch. Ott, A. Albu-Schäffer, A. Kugi, and G. Hirzinger, "On the passivity based impedance control of flexible joint robots," *IEEE Transactions on Robotics*, vol. 24, no. 2, pp. 416–429, 2008.

[18] J. de Jalon and E. Bayo, *Kinematic and Dynamic Simulation of Multibody Systems: The Real-Time Challenge*, ser. Mechanical Engineering Series. Springer-Verlag, 1994.

[19] H. K. Khalil, *Nonlinear Systems*, 3rd ed. Prentice Hall, 2002.

[20] A. van der Schaft, *L_2-Gain and Passivity Techniques in Nonlinear Control*, 2nd ed. Springer-Verlag, 2000.

[21] J. Park, W. Chung, and Y. Youm, "On dynamical decoupling of kinematically redundant manipulators," in *IEEE/RSJ Int. Conf. on Intelligent Robots and Systems*, 1999, pp. 1495–1500.

[22] Ch. Ott, A. Kugi, and Y. Nakamura, "Resolving the problem of non-integrability of nullspace velocities for compliance control of redundant manipulators by using semi-definite lyapunov functions," in *IEEE Int. Conf. on Robotics and Automation*, 2008, pp. 1999–2004.

[23] A. Albu-Schäffer, Ch. Ott, U. Frese, and G. Hirzinger, "Cartesian impedance control of redundant robots: Recent results with the dlr-light-weight-arms," in *IEEE Int. Conf. on Robotics and Automation*, 2003, pp. 3704–3709.